



Universiteit
Leiden
The Netherlands

15N Photo-CIDNP MAS NMR To Reveal Functional Heterogeneity in Electron Donor of Different Plant Organisms

Janssen, G.J.; Roy, E.; Matysik, J.; Alia, A.

Citation

Janssen, G. J., Roy, E., Matysik, J., & Alia, A. (2012). 15N Photo-CIDNP MAS NMR To Reveal Functional Heterogeneity in Electron Donor of Different Plant Organisms. *Applied Magnetic Resonance*, 42(1), 57-67. doi:10.1007/s00723-011-0283-8

Version: Not Applicable (or Unknown)

License: [Leiden University Non-exclusive license](#)

Downloaded from: <https://hdl.handle.net/1887/61018>

Note: To cite this publication please use the final published version (if applicable).

¹⁵N Photo-CIDNP MAS NMR To Reveal Functional Heterogeneity in Electron Donor of Different Plant Organisms

Geertje J. Janssen · Esha Roy · Jörg Matysik · A. Alia

Received: 19 July 2011 / Revised: 31 August 2011 / Published online: 15 November 2011
© The Author(s) 2011. This article is published with open access at Springerlink.com

Abstract In plants and cyanobacteria, two light-driven electron pumps, photosystems I and II (PSI, PSII), facilitate electron transfer from water to carbon dioxide with quantum efficiency close to unity. While similar in structure and function, the reaction centers of PSI and PSII operate at widely different potentials with PSI being the strongest reducing agent known in living nature. Photochemically induced dynamic nuclear polarization (photo-CIDNP) in magic-angle spinning (MAS) nuclear magnetic resonance (NMR) measurements provides direct access to the heart of large photosynthetic complexes (A. Diller, Alia, E. Roy, P. Gast, H.J. van Gorkom, J. Zaanen, H.J.M. de Groot, C. Glaubitz, J. Matysik, *Photosynth. Res.* 84, 303–308, 2005; Alia, E. Roy, P. Gast, H.J. van Gorkom, H.J.M. de Groot, G. Jeschke, J. Matysik, *J. Am. Chem. Soc.* 126, 12819–12826, 2004). By combining the dramatic signal increase obtained from the solid-state photo-CIDNP effect with ¹⁵N isotope labeling of PSI, we were able to map the electron spin density in the active cofactors of PSI and study primary charge separation at atomic level. We compare data obtained from two different PSI proteins, one from spinach (*Spinacia oleracea*) and other from the aquatic plant duckweed (*Spirodella oligorrhiza*). Results demonstrate a large flexibility of the PSI in terms of its electronic architecture while their electronic ground states are strictly conserved.

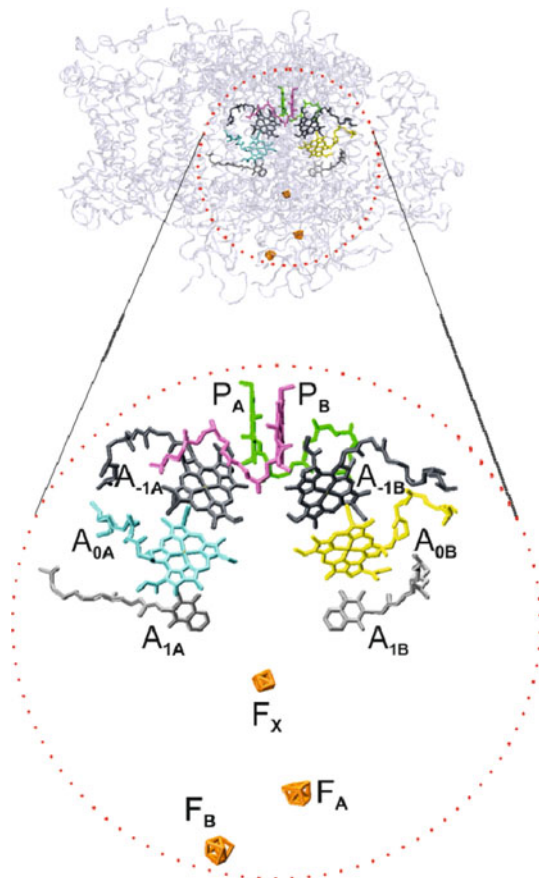
1 Introduction

Photosynthesis in cyanobacteria, algae and plants involves the participation of two reaction centers (RCs), photosystem I (PSI) and photosystem II (PSII), located in the thylakoid membrane of chloroplasts. The coupling of these two photosystems allows for pumping electrons across the photosynthetic membrane from water

G. J. Janssen · E. Roy · J. Matysik · A. Alia (✉)
Leiden Institute of Chemistry, Leiden University, P.O. box 9502, 2300 RA Leiden, The Netherlands
e-mail: a.alia@chem.leidenuniv.nl

molecules finally into CO_2 in order to build up organic material. The oxidized primary electron donor of PSII, $\text{P680}^{+\cdot}$, is the strongest oxidizing agent known in living nature, having a redox potential of at least 1.2 V [3]. On the other hand, the electronically excited electron donor of PSI, P700, is a strongly reducing agent, having a potential of approximately -1.2 V. Thus, P700^* probably is the most reducing compound found in natural systems [4]. The redox properties of PSI are highly optimized to provide a strongly reducing force. The X-ray structure of cyanobacterial PSI has been solved with 2.5 Å resolution and shows high resemblance to plant PSI [5, 6]. From plant PSI currently only X-ray structures of near-atomic resolution (down to 3.4 Å [7]) are available, leaving the exact electronic structure of plant P700 a matter of debate. All PSI systems, as other RCs, have two symmetric branches consisting of six chlorine molecules and two quinones (Fig. 1). Furthermore, PSI contains three iron–sulphur [4Fe–3S] clusters as terminal intrinsic electron acceptors [8]. The primary electron donor P700 is a heterodimer consisting of one chlorophyll *a* (Chl *a*, P_B) and one Chl *a'* (P_A) which is the 13^2 -epimer of Chl *a*. While P_A forms hydrogen bonds to its protein environment, no hydrogen bonds are found on the P_B side [5]. Electron paramagnetic resonance

Fig. 1 Arrangement of the cofactors in the RC of PSI (*bottom*) located in the heart of the PSI protein (*top*). Based on the X-ray crystal structure of cyanobacterial PSI [5], visualized using VMD (Beckman Institute, University of Illinois at Urbana-Champaign)



(EPR) studies showed most of the positive charge to be localized on the Chl *a* (the P_B donor) molecule [9, 10], however, a consensus about the extent of asymmetry has not been reached yet [2, 11].

In contrast to PSII where electron transfer (ET) is known to be primarily on a single branch, data from transient EPR implied both branches to be active in PSI [12–14]. However, the conservation of the occurrence of bidirectional ET among different species and varying experimental conditions remains under discussion [11]. The biological significance of bidirectional ET in PSI is also not yet understood. Hence, despite the highly optimized redox properties of P700, PSI appear to be functionally heterogeneous, e.g., in terms of (relative) participation of the two branches in ET. The question arises whether these functional variations affect P700 or remain in the periphery. Of special interest would be a comparison of plant systems, containing the highest evolved photosystems, from different habitats.

Photochemically induced dynamic nuclear polarization (photo-CIDNP) is well known in liquid nuclear magnetic resonance (NMR) as a method that increases the NMR intensities [15, 16]. In solid-state NMR upon illumination with continuous white light, photo-CIDNP has been observed by applying ^{15}N magic-angle spinning (MAS) NMR to four photosynthetic RCs: (i) *Rhodobacter (R.) sphaeroides* R26 [17–20], wild type (WT) [21–23], PSI [2, 24], and PSII [24]. Photo-CIDNP is caused by the strong electron polarization in the initial radical pair and subsequently transferred to nuclei, where it is detected by NMR as a signal enhancement up to a factor of about 10,000 [25, 26]. The origin of photo-CIDNP in bacterial RCs is now understood [27, 28]. Two coherent mechanisms running in parallel, called “three spin mixing” and “differential decay”, transfer electron spin order to nuclear spin order. The third mechanism, called “cyclic reaction” or “differential decay”, requires long lifetime of the donor triplet state and is not expected to be relevant in PSI. Since the appearance of the photo-CIDNP signals improves the sensitivity and selectivity of NMR dramatically, this method allows studying small changes in the photochemically active region of the RCs in great detail and is therefore particularly suitable for the study of environmental effects on P700. In this study we compare PSI proteins of spinach (*Spinacia oleracea*) and of the aquatic plant duckweed (*Spirodela oligorhiza*), using ^{15}N photo-CIDNP MAS NMR. Our results demonstrate that electronic ground state of the donor is highly conserved despite flexibility of electronic architecture in two different plant systems.

2 Materials and Methods

2.1 PSI Particle Preparation

^{15}N -labelled spinach (*Spinacia oleracea*) plants were grown as described by Diller et al. [24]. ^{15}N -labelled duckweed (*S. oligorhiza*) plants were grown under aseptic conditions on half-strength Hunter’s medium [29] under continuous light ($20 \mu\text{Em}^{-2}\text{s}^{-1}$) at 25°C . The medium was continuously bubbled with sterile air containing 5% CO_2 . As the source of isotope-labeled nitrogen KNO_3 was substituted by 5.5 mM of $^{15}\text{NH}_4^{15}\text{NO}_3$, furthermore $\text{Ca}(\text{NO}_3)\cdot 4\text{H}_2\text{O}$ was replaced

by 4 mM CaCl_2 . After 7 days plants were harvested, frozen in liquid nitrogen and stored at -80°C until use. The PSI complex containing ~ 110 Chl/P700 (PSI-110 particles) was prepared according to the method described by Alia et al. [2].

2.2 Photo-CIDNP MAS NMR Experiments

The NMR experiments were performed on DMX-100, -200, -300 and -400 NMR spectrometers (Bruker GmbH, Karlsruhe, Germany). The samples were loaded into optically transparent 4 mm sapphire rotors. The PSI samples were reduced by the addition of an aqueous solution of 10 mM sodium dithionite and 40 mM glycine buffer (pH 9.5) in an oxygen-free atmosphere. Immediately following the reduction, slow freezing of the sample was performed directly in the NMR probe inside the magnet with liquid nitrogen-cooled gas under continuous illumination with white light. Temperature was kept at 235 K. The illumination setup used was specially designed for the Bruker MAS probe [30]. The light and dark spectra were obtained with a pulse-echo pulse sequence and two pulse phase modulation (TPPM) proton decoupling. The number of scans was 20 k, unless stated differently. The fitting of the collected spectra was performed using Igor Pro 6.01. On the basis of the relative intensity of the signals, the electron spin density (ESD) was calculated for the nitrogen assigned to the donor.

3 Results and Discussion

3.1 The Occurrence of Photo-CIDNP in Different Plant PSI

Figure 2a shows the ^{15}N MAS NMR spectrum of uniformly ^{15}N -labeled PSI of duckweed obtained under continuous illumination. The very weak and broad positive signals arising at about 120 ppm originate from amide nitrogen of protein backbone and are also present in spectra obtained under dark conditions (data not shown). Upon illumination six absorptive (positive) and five emissive (negative) photo-CIDNP signals can be resolved in the spectrum. No spinning side bands are observed at the applied magnetic field (4.7 T) and spinning speed (8 kHz). The narrow line width of the photo-CIDNP signals is in line with the expected high rigidity and order within the RC. Previously, the photo-CIDNP effect in PSI has been shown in another plant, spinach [1, 2, 31], as well as in *Synechocystis* [32]. Here, we demonstrate that the solid-state photo-CIDNP effect on PSI can also be observed in duckweed. Hence, it appears that the effect occurs in all natural photosynthetic systems [33]. Being an aquatic plant, duckweed has the advantage over spinach, since it is easier to introduce isotope labels [34] which would allow for more detailed and selective ^{15}N and ^{13}C solid-state photo-CIDNP studies in the future. Duckweed already has shown to successfully incorporate isotope-labeled amino acids into its RC [34]. Further work in that direction is currently at progress in our laboratory.

Spectra a and b in Fig. 2 compare the ^{15}N MAS NMR spectrum of uniformly ^{15}N -labeled PSI of duckweed and spinach obtained under continuous illumination, with light-induced signals occurring between 180 and 280 ppm. Figure 3 shows

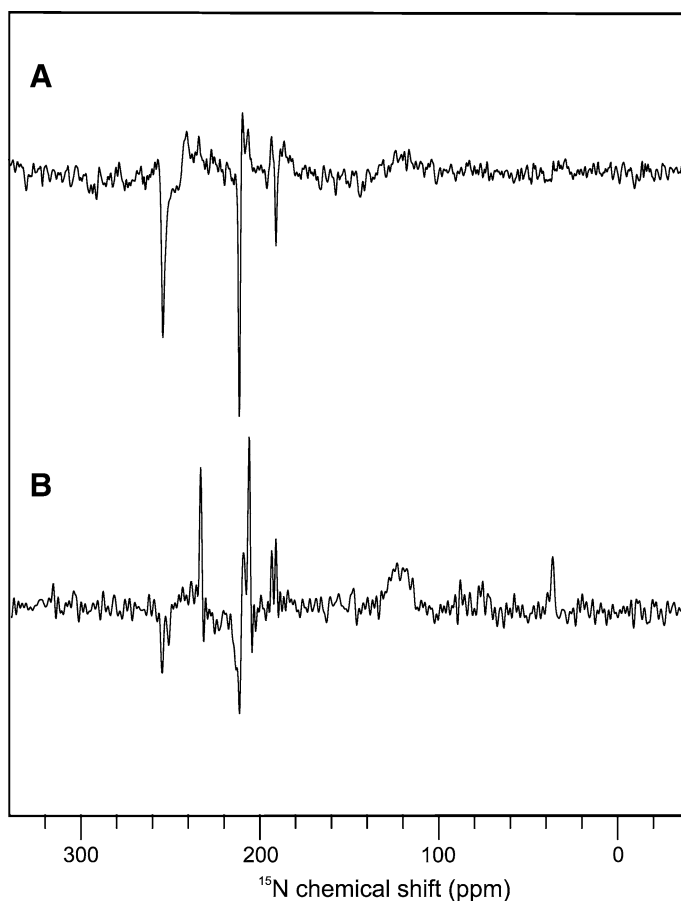


Fig. 2 ^{15}N photo-CIDNP MAS NMR overview spectra of PSI of duckweed (**a**) and spinach (**b**), obtained under continuous illumination at 9.4 T and 240 K with a cycle delay of 4 s

detailed spectra of duckweed (Fig. 3a) and spinach (Fig. 3b) PSI. Both the line width and the chemical shift of the photo-CIDNP signals observed in the two different plant systems are very similar. However, major differences are observed in terms of signal intensity and sign.

3.2 Signal Assignment and the Electron Spin Density Distribution in the Primary Donor P_B

The ^{15}N chemical shifts assignment of the photo-CIDNP signals observed in duckweed PSI are given in Table 1, and are compared with ^{15}N chemical shifts assignment of spinach PSI [24] and liquid MAS NMR data of free Chl *a* in solution [35].

If both branches participate in the ET, photo-CIDNP signals from up to three active Chl *a* and one active Chl *a'* cofactors can be expected from PSI with a total

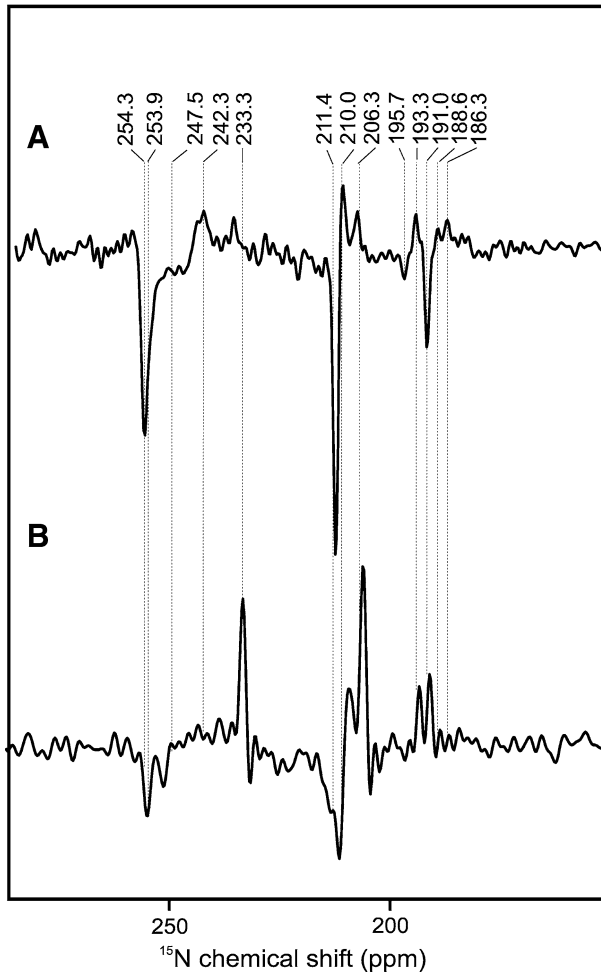


Fig. 3 Detailed ^{15}N photo-CIDNP MAS NMR spectra of the light-induced signals obtained from PSI of duckweed (a) and spinach (b), obtained under continuous illumination at 9.6 T and 240 K with a cycle delay of 4 s

maximum of sixteen nitrogen. In photo-CIDNP spectra of PSI in duckweed, a total of 11 signals have been observed, opposed to 8 signals assigned previously based on the data obtained from spinach PSI [1]. In duckweed PSI the four signals observed between 242 and 255 ppm have been assigned to the N-IV nitrogen of four different cofactors. In addition, the observation of three signals within the chemical shift region expected for N-II nitrogen indicates that both the branches may be active in PSI of duckweed. Based on the expectation that most ESD is located on the primary Chl *a* donor of the B-branch (P_B) [36], four signals in the spectrum obtained from duckweed PSI have been assigned to the nitrogen of P_B : N-I at 186.3 ppm, N-II at 211.4 ppm, N-III at 191.0 ppm and N-IV at 254.3 ppm (bold printed in Table 1). The signal at 186.3 ppm (Fig. 3) which is assigned to the N-I of P_B (Table 1) is

Table 1 ^{15}N chemical shifts of the photo-CIDNP signals observed in duckweed in comparison with published chemical shift data

Atom assignment	Solution data $\sigma_{\text{liq}}^{\text{a}}$	PSI spinach $\sigma_{\text{solid}}^{\text{b}}$	PSI duckweed $\sigma_{\text{solid}}^{\text{c}}$
N-I	186.0	186.2 (e)	186.3 (a)
		190.9 (a)	188.6 (a)
N-II	206.5	206.1 (a)	206.3 (a)
		211.5 (e)	211.4 (e)
N-III	189.4	193.2 (a)	191.0 (e)
		193.3 (a)	193.3 (a)
N-IV	247.0	233.3 (a)	242.3 (a)
		250.3 (e)	247.5 (e)
		254.9 (e)	254.3 (e)

All shifts are referenced to liquid ammonia with use of an external standard of solid $^{15}\text{NH}_4\text{NO}_3$ ($\delta = 23.5$). Bold printed shifts are assigned to the primary Chl *a* donor of the B-branch (P_B)

a Absorptive (positive), *e* emissive (negative)

^a Chemical shift in ppm. Measured in CDCl_3 . Source: [35]

^b Chemical shift in ppm. Source: [24, 39]

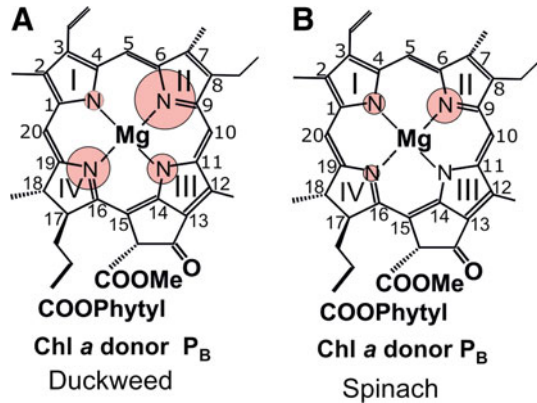
^c Chemical shift in ppm. Source: this work

absorptive in duckweed and emissive in spinach while, in general, the absorptive signals observed in spinach PSI spectrum are much more pronounced. The relative intensities of the emissive signals assigned to the P_B cofactor are higher in duckweed compared with respective signals observed in spinach.

Comparing the chemical shifts observed in duckweed with those observed in spinach (Fig. 3) [24], similar transitions are observed (Table 1). Such finding is expected because in all cases, both donor and primary acceptor cofactors consist of plant Chl *a* (and Chl *a'*). Hence, our data imply that there is nothing unusual in RCs of duckweed concerning the cofactors and their electronic ground state.

Based on the intensities of the observed photo-CIDNP signals, the ESD distribution in the $2p_z$ orbitals can be estimated (for details, see Ref. [1]). In Fig. 4 the ESD map of the P_B cofactor of duckweed (Fig. 4a) is compared to the relative ESD distribution observed in the primary donor of spinach PSI (Fig. 4b). Both in duckweed and in spinach, most ESD is located on the ring II nitrogen, which is in line with the ESD distribution observed for free Chl *a* in solution [10, 37, 38]. Likewise similar to undisturbed Chl *a* in solution, little ESD is observed on N-I in both spinach and duckweed PSI. A prominent difference is that the signal assigned to the ring I nitrogen of P_B of spinach (at 186.2 ppm) is emissive in nature while in duckweed it is observed as an absorptive signal at almost the exact chemical shift (186.3 ppm, Table 1; Fig. 3). Compared to spinach PSI a much higher ESD on the ring IV nitrogen is observed in duckweed PSI (Fig. 4a) while a moderate ESD is found to be located on N-III. None of the signals in the spectrum obtained from

Fig. 4 ESD patterns of the primary donor of the B branch (P_B) of PSI of duckweed (**a**) and spinach (**b**) based on the ^{15}N photo-CIDNP intensities



spinach PSI (Table 1; Fig. 3b) was assigned to the N-III of the primary donor P_B which is expected as an emissive signal around 190 ppm (Table 1) [24].

In contrast to the high similarity in chemical shifts, the intensity patterns between duckweed and spinach appear to be substantially different. Such dramatic changes in the intensity pattern suggest fundamental differences between the radical pairs in both plant systems. One might assume that this difference is caused by another balance of the enhancement mechanisms. That would imply that parameters ruling dynamics or architecture of the radical pair are different. Such an interpretation implies that there is a large flexibility in PSI systems as proposed earlier [11]. One could imagine, for example, the occurrence of not only dimeric donor cation-radicals but also double radical anions from both branches. The differences in the electronic architecture may also be due to different patterns of activation of two branches in two systems leading to more asymmetric radical pair architectures having other coupling parameters.

3.3 The Magnetic Field Effect of Photo-CIDNP in Different Plant PSI

The field dependence of the solid-state photo-CIDNP effect in PSI from spinach has been measured previously [31] and it was shown that the effect decays at high fields having a maximum at about 9.4 T. Figure 5 shows the relative signal-to-noise intensity of the photo-CIDNP signals obtained from uniformly ^{15}N -labeled PSI of duckweed (Fig. 5a) and spinach (Fig. 5b) at different magnetic field strengths. In line with previous observations in spinach PSI [31], the light-induced signals of duckweed PSI increase in intensity with an increasing magnetic field strength from 2.4 T up to 9.4 T. Within the limited range of the observed fields, the field dependence of the solid-state photo-CIDNP effect in duckweed seems to be similar to that in spinach (Fig. 5). Such an observation would be rather puzzling since the significant differences in the intensity patterns of the light-induced signals suggest different electronic architecture of the radical pairs, while the field dependence appears to be similar in the two systems.

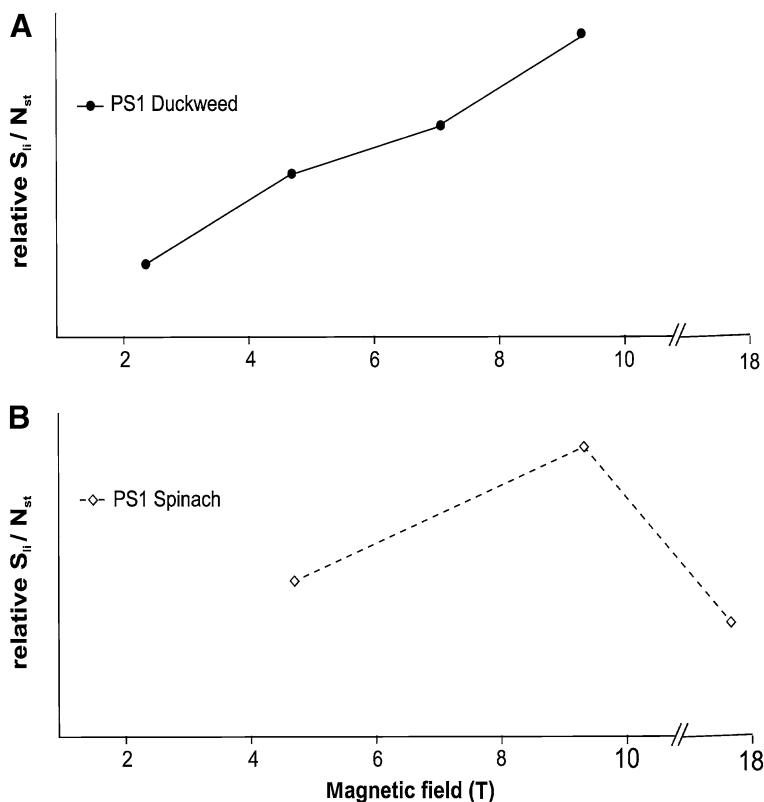


Fig. 5 Relative magnitude of the ratio of light-induced signal (S_i) to the standardized noise (N_{st}) for PS1 of duckweed (a) and spinach (b) [31]

4 Outlook

Further experimental and theoretical studies are on the way in our laboratory aiming to assign the signals to the different cofactors in the two branches and to explain the differences between the radical pairs in the two PSI systems. In particular, ^{13}C , ^{15}N selective isotope labeling might allow for proper signal assignment allowing for solid theoretical simulation. Time-resolved experiments and complete field-dependent data might reveal the origin of the different intensity patterns.

Acknowledgments We thank Prof. G. Jeschke, Prof. H.J.M. de Groot and Dr. B. Bode for helpful discussions. The help of F. Lefeber, K.B. Sai Sankar Gupta, and K. Erkelens is gratefully acknowledged. This work was financially supported by the Aard- en levenswetenschappen (ALW) grant 818.02.019 to J.M. and by the Foundation for Fundamental Research on Matter (FOM) grant 10TBSC23 to A.A.

Open Access This article is distributed under the terms of the Creative Commons Attribution Non-commercial License which permits any noncommercial use, distribution, and reproduction in any medium, provided the original author(s) and source are credited.

References

1. A. Diller, Alia, E. Roy, P. Gast, H.J. van Gorkom, J. Zaanen, H.J.M. de Groot, C. Glaubit, J. Matysik, *Photosynth. Res.* **84**(1–3), 303–308 (2005)
2. Alia, E. Roy, P. Gast, H.J. van Gorkom, H.J.M. de Groot, G. Jeschke, J. Matysik, *J. Am. Chem. Soc.* **126**(40), 12819–12826 (2004)
3. H.J. Gorkom, J.P.M. Schelvis, *Photosynth. Res.* **38**, 297–301 (1993)
4. A.N. Webber, W. Lubitz, *Biochim. Biophys. Acta* **1507**(1–3), 61–79 (2001)
5. P. Jordan, *Nature* **411**(6840), 909–917 (2001)
6. P. Fromme, P. Jordan, N. Krauss, *Biochim. Biophys. Acta* **1507**(1–3), 5–31 (2001)
7. A. Amunts, H. Toporik, A. Borovikova, N. Nelson, *J. Biol. Chem.* **285**(5), 3478–3486 (2009)
8. S.P. Romberger, J.H. Golbeck, *Photosynth. Res.* **104**(2–3), 333–346 (2010)
9. A.R. Holzwarth, *Biophys. J.* **90**(2), 552–565 (2006)
10. H. Kass, J. Rautter, B. Bonigk, P. Hofer, W. Lubitz, *J. Phys. Chem.* **99**(1), 436–448 (1995)
11. S. Santabarbara, I. Kuprov, O. Poluektov, A. Casal, C. Russel, S. Purton, M.C.W. Evans, *J. Phys. Chem. B* **114**(46), 15158–15171 (2010)
12. P. Setif, K. Brettel, *Biochemistry* **32**(31), 7846–7854 (1993)
13. O.G. Poluektov, S.V. Paschenko, L.M. Utschig, K.V. Lakshmi, M.C. Thurnauer, *J. Am. Chem. Soc.* **127**(34), 11910–11911 (2005)
14. M.G. Muller, C. Slavov, R. Luthra, K.E. Redding, A.R. Holzwarth, *Proc. Natl. Acad. Sci. USA* **107**(9), 4123–4128 (2010)
15. P.J. Hore, R.W. Broadhurst, *Prog. Nucl. Magn. Reson. Spectrosc.* **25**, 345–402 (1993)
16. M. Goetz, in *Advance in Photochemistry*, ed. by D.C. Neckers, D.H. Volman, G. von Büнау (Wiley, New York, 1997), pp. 63–163
17. S. Prakash, Alia, P. Gast, H.J.M. de Groot, J. Matysik, G. Jeschke, *J. Am. Chem. Soc.* **128**(39), 12794–12799 (2006)
18. M.G. Zysmilich, A. McDermott, *J. Am. Chem. Soc.* **116**(18), 8362–8363 (1994)
19. M.G. Zysmilich, A. McDermott, *J. Am. Chem. Soc.* **118**(25), 5867–5873 (1996)
20. J. Matysik, *Proc. Natl. Acad. Sci. USA* **97**(18), 9865–9870 (2000)
21. E.A.M. Schulten, J. Matysik, Alia, S. Kiihne, J. Raap, J. Lugtenburg, P. Gast, A.J. Hoff, H.J.M. de Groot, *Biochemistry* **41**(27), 8708–8717 (2002)
22. S. Prakash, Alia, P. Gast, H.J.M. de Groot, G. Jeschke, J. Matysik, *J. Am. Chem. Soc.* **127**(41), 14290–14298 (2005)
23. E. Daviso, S. Prakash, A. Alia, P. Gast, G. Jeschke, J. Matysik, *Appl. Magn. Reson.* **37**(1–4), 49–63 (2010)
24. A. Diller, E. Roy, P. Gast, H.J. van Gorkom, H.J.M. de Groot, C. Glaubit, G. Jeschke, J. Matysik, A. Alia, *Proc. Natl. Acad. Sci. USA* **104**(31), 12767–12771 (2007)
25. S. Prakash, Alia, P. Gast, H.J.M. de Groot, G. Jeschke, J. Matysik, in *Photosynthesis: Fundamental Aspect to Global Perspectives*, ed. by A. van der Est, A. Bruce (Allen Press, Montréal, 2005), pp. 301–302
26. S. Prakash, *Photo-CIDNP studies on reaction centers of Rhodobacter sphaeroides*, PhD Thesis, Universiteit Leiden, Leiden (2006)
27. J. Matysik, G. Jeschke, *Chem. Phys.* **294**, 239–255 (2003)
28. E. Daviso, S. Prakash, A. Alia, P. Gast, J. Neugebauer, G. Jeschke, J. Matysik, *Proc. Natl. Acad. Sci. USA* **106**, 22281–22286 (2009)
29. H.B. Posner, in *Methods in Developmental Biology*, ed. by F.A. Wilt, S.N.K. Wessel (Crowell, New York, 1967), pp.131–317
30. J. Matysik, Alia, J.G. Hollander, T. Egorova-Zachernyuk, P. Gast, H.J.M. de Groot, *Indian J. Biochem. Biophys.* **37**(6), 418–423 (2000)
31. E. Roy, A. Diller, Alia, P. Gast, H.J. van Gorkom, H.J.M. de Groot, G. Jeschke, J. Matysik, *Appl. Magn. Reson.* **31**(1–2), 193–204 (2007)
32. G.J. Janssen, E. Daviso, M. van Son, H.J. de Groot, A. Alia, J. Matysik, *Photosynth. Res.* **104**(2–3), 275–282 (2010)
33. J. Matysik, A. Diller, E. Roy, A. Alia, *Photosynth. Res.* **104**, 427–435 (2009)
34. B. Alia, *Chem. Phys.* **294**(3), 459–469 (2003)
35. S.G. Boxer, G.L. Closs, J.J. Katz, *J. Am. Chem. Soc.* **126**, 7058–7066 (1974)
36. M. Plato, *Chem. Phys.* **294**(3), 483–499 (2003)

37. H. Kass, P. Fromme, W. Lubitz, *Chem. Phys. Lett.* **257**(1–2), 197–206 (1996)
38. H. Kass, W. Lubitz, G. Hartwig, H. Scheer, D. Noy, A. Scherz, *Spectrochimica Acta Part A* **54**(9), 1141–1156 (1998)
39. G. Jeschke, J. Matysik, *Chem. Phys.* **294**(3), 239–255 (2003)